

Study on Upper Air Sounding Data Sensitivity towards Thunderstorm Activities over Kuching and Miri from 2010 to 2015

Kajian Sensitiviti Pencerapan Udara Atas terhadap Aktiviti Ribut Petir di Kuching dan Miri dari tahun 2010 hingga 2015

NOOR AZAM BIN SHAARI¹, NOOR AZRA BINTI AHIM, PHUANG ENG BENG , SITI AIZZA BINTI SARMANI, ALLISCIA ANAK MANDAI, NOOR FATEEN A'DILA BINTI ABDUL SHUKUR & MOHD KHAIRUL IKHWAN BIN MOHD ZAWAWI

¹ Malaysian Meteorological Department

*Corresponding author: Noor Azam Shaari (azam@met.gov.my)

Published online:

To cite this article (APA): Noor Azam, S., Noor Azra, A., Phuah, E. B., Siti Aizza, S., Alliscia, A.M., Noor Fateen A'dila, A. S. & Mohd Khairul Ikhwan, M.Z. (2020). Study on Data Sounding Sensitivity towards Thunderstorm Activities over Kuching and Miri from 2010-2015. *GEOGRAFI*, 8(1), 1-24.

ABSTRACT *Severe thunderstorm and rainfall activities are dangerous to any humankind activities including the airport operations. Thorough studies about the thunderstorm activities at the airports are important for flight safety as scholars have attempted to understand thunderstorm behavior that is measured from atmospheric stability indices. The atmospheric stability indices at Kuching and Miri airports were analyzed to predict the precursor of the phenomenon and to improve the forecasting skills among the forecasters. The result shows that the stability indices suggested by the models were found not to be exclusive to represent the phenomenon that had occurred at some points. The phenomenon might not occur at all, although the index falls within the suggested model's range. A linear relationship between any two models was analyzed to observe how they interact between them. A strong negative linear relationship between SI -TTI and CAPE-LI was found negative while TPW-KI was in a positive correlation coefficient value. The presence of the water content measured by TPW may provide some information about the precursor of the phenomenon at the airports. The index was found to be concentrated at some points during the phenomenon. Thus, TPW may be useful as the third indices to support the relationship between SI-TTI and CAPE-LI as thunderstorm predictions are made at the airports in the future.*

Keywords: Thunderstorms, Phenomenon, Atmospheric Stability Indices, Correlation Coefficient

ABSTRAK *Aktiviti ribut petir dan hujan lebat adalah sangat merbahaya kepada semua aktiviti manusia termasuk operasi penerbangan. Kajian saintifik mengenai fenomena cuaca yang berlaku di lapangan terbang utama adalah sangat penting dalam menjamin kelancaran aktiviti penerbangan serta dalam memahami sifat kejadian fenomena yang diukur melalui indeks kestabilan atmosfera.*

Tahap indeks kestabilan atmosfera untuk dua lapangan terbang utama di Sarawak iaitu di Kuching dan Miri dikaji agar ianya dapat digunakan sebagai penanda aras terhadap kewujudan fenomena ini, seterusnya membantu meningkatkan kualiti dan ketepatan ramalan yang dikeluarkan oleh pengamal kajicuaca. Hasil kajian mendapati tahap indeks kestabilan yang dicadangkan melalui beberapa model antarabangsa adalah tidak eksklusif kepada kewujudan fenomena pada satu-satu masa. Ribut petir tidak semestinya berlaku walaupun ianya sepadan dengan model yang dicadangkan. Hubungan linear antara dua model telah dilakukan bagi melihat interaksi antara mana-mana dua model. Hubungan linear antara model SI-TTI dan CAPE-LI mendapati bahawa pekali korelasi bersifat negatif manakala TPW-LI bersifat positif. Kehadiran kandungan wap air di dalam atmosfera yang diukur melalui model TPW didapati dapat memberi gambaran awal mengenai kehadiran fenomena. Kajian mendapati bahawa ketumpatan indeks terfokus kepada indeks tertentu semasa kejadian fenomena. Justeru itu, TPW boleh dijadikan sebagai model indeks ketiga untuk digunakan bersama antara dua model SI-TTI atau CAPE-LI apabila meramal fenomena ribut petir di lapangan terbang pada masa hadapan.

Kata kunci: Ribut Petir, Fenomena, Indeks Kestabilan Atmosfera, Pekali Korelasi

1. Introduction

Thunderstorm is one of the significant meteorological phenomena occurring in Malaysia and that becomes severe during the inter-monsoon season in April and October each year. There are two major parts of this country- the Peninsula Malaysia to the west and East Malaysia to the east. Due to the geographical boundary separated by the South China Seas, the climate is slightly different from one another. The main reason for the severe thunderstorm during this monsoon is due to the presence of light wind and the varying direction. The presence of light and the various winds usually will cause active clouds to be formed over the region.

Other than thermal heating and the presence of equatorial trough, many other factors promote severe thunderstorms such as atmospheric instability, lift and moisture content (Gottlieb & Wyosocki, 2009). Thunderstorm generation is mainly governed by the thermodynamic conditions of the atmosphere (Bhattacharya et al., 2011). The clouds have to pass through a few stages before they become active and finally manifested as thunderstorms and in some occasions followed with rain. The developing stage of thunderstorms begins when the cumulus clouds are being pushed upward by a rising column of air (updraft) (<http://www.nssl.noaa.gov/education/svrwx101/thunderstorms/>) during the convection process. The warm air in an updraft trough will continue to rise until its

maturity stage where the air reaches the tropopause layer and will form characteristics like an anvil shape. The anvil form of shape will extend the furthest in a direction as blown by the upper-tropospheric winds (Stull, 2017). While the process continues, the falling rain will create downdrafts together with the storms. As the downdraft hits the ground, the precipitation will be weakening, and the air and its surroundings will be cooled and become more stable. Severe thunderstorm and heavy rain are usually associated with a strong downdraft and usually dangerous to humankind. Hence, monitoring the atmospheric condition is important to predict the thunderstorm on that day.

The purpose of the study is to evaluate the thunderstorm activities and patterns over meteorological stations in Kuching (WBGG) and Miri (WBGR). The stability index during the Thunderstorm and Rain (TSRA) days at both meteorological stations is analyzed in order to understand the phenomenon hence, to improve the forecasting techniques and skills. Forecasting TSRA using a single stability index may not be effective because the atmospheric stability is always influenced by its dynamic atmospheric conditions. Hence, more options of the stability index are required and should be analyzed parallel to the evaluation of the current atmospheric situations for making prediction. The relationship between each index that induces thunderstorm is evaluated and the result is suggested to be used as a forecasting guideline. This is the first attempt of a project research to observe the behavior of all stability indices towards the thunderstorms activities over Kuching and Miri.

2. Methodology

A vertical atmospheric profile for the selected area is monitored in order to measure the atmospheric condition over the region. The vertical profiles or upper air parameters such as the temperature, humidity, wind speed, wind direction, geopotential height and atmospheric pressure are observed using a meteorological device named Radiosonde. The device is tethered to a balloon and launched from each meteorological station twice daily. According to the National Centers for Environmental Information of National Oceanic and Atmospheric Administration (NOAA), more than 1500 radiosonde and pilot balloons are released to observe the meteorological parameters globally. The radiosonde can ascend to an altitude of more than 35 km (about 115,000 feet) and drift to more than 300 km (about 180 miles) from the released stations (<http://www.weather.gov/upperair/factsheet>). All the important parameters are immediately measured from the three meters of the

earth's surface and up to the stratosphere layer. While ascending through the troposphere and stratosphere, the data is then transmitted back to the receiving stations on the ground. Various stability indices will be generated to indicate the current atmospheric condition to predict the thunderstorms. The weather balloons are released from the selected meteorological stations in Malaysia as shown in Figure 1. The stations are also responsible for monitoring all the meteorological parameters on the ground following the guideline issued by the World Meteorological Organizations (WMO). The weather balloon station from Brunei (WBSB) is used to represent the atmospheric conditions over Miri (WBGR) as the station does not provide the parameters. The distance between both stations is about 160 km from each other.

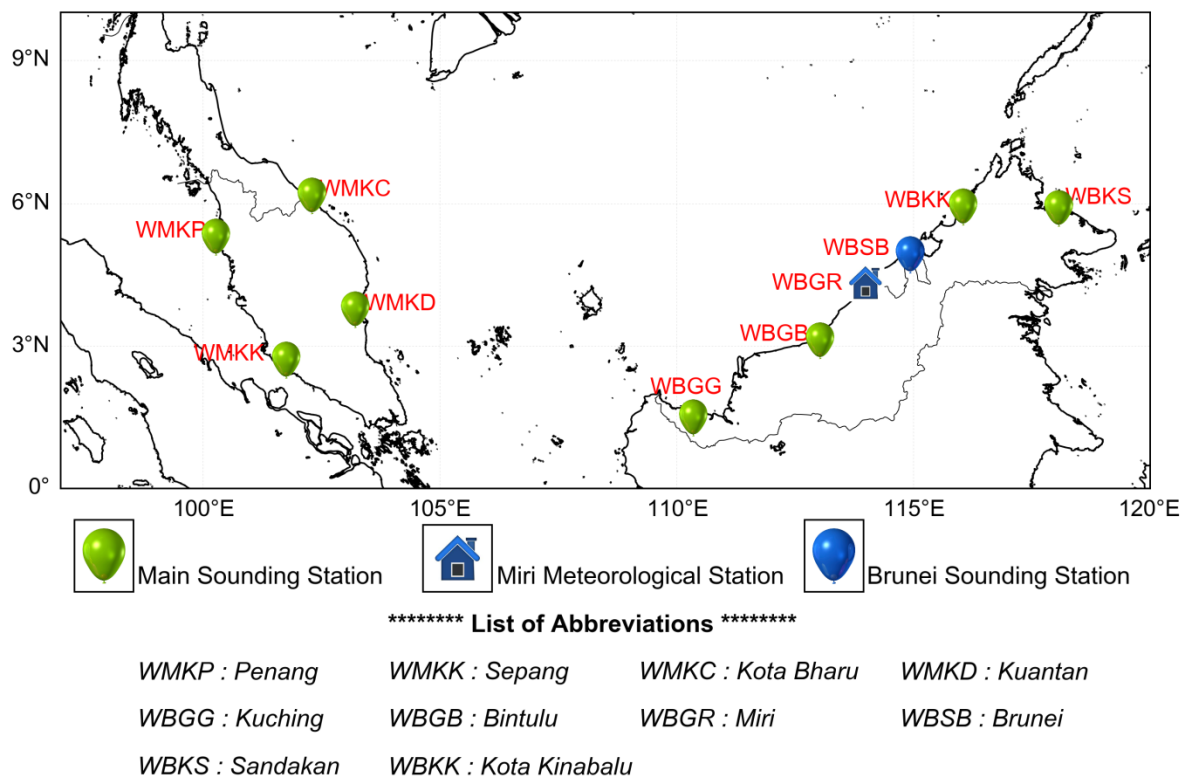


Figure 1. Meteorological stations in Malaysia

The index generated by the radiosonde is generally used to describe the atmospheric stability at the respective region. The index is found to be an effective forecasting tool to predict the potential thunderstorms and frequently used as the guideline in Malaysian Meteorological Department (2009), and a similar concept of theory and methodology from the previous research by Shaari et al. (2015) is applied

in this study. The static stability index such as K Index by George (1960), Lifting Index by Galway (1956), Showalter Index by Showalter (1953) and Total Totals Index by Miller (1967) were thoroughly reviewed in detail by Peppler (1988) and became a guide in the study. There are many types of indices that have been developed in order to understand the phenomenon while improving the forecasting skills.

2.1 K-Index

K-Index (KI) is used to forecast the non-severe thunderstorm activities and arithmetically combines the 850hpa to 500hpa temperature difference, the 850hpa dew-point (a direct measure of low-level moisture content), and the 700hpa dew-point depression (an indirect measure of the vertical extent of the moist layer) to help forecast the potential continental summertime air mass thunderstorm (Peppler, 1988). The KI is formularized as $KI = [T(850hPa) - T(500hPa)] + T_d(850hPa) - [T(700hPa) - T_d(700hPa)]$. Where, T and T_d represent the temperature and dew point temperature at the indicated level. The air mass thunderstorm is referred to those developing in the areas of weak winds without apparent frontal or cyclonic influence (George, 1960). The summary of KI range that gives an indication of the possibility of thunderstorm forming over the region is described in Table 1.

Table 1. KI criteria index range

KI	Thunderstorm Potential
< 20	20% Unlikely
21 – 25	20 – 40% Isolated Thunderstorms
26 – 30	40 – 60% Thunderstorms
31 – 35	60 – 80% Widely Scattered Thunderstorms
36 – 40	80 – 90% Numerous Thunderstorms
> 40	Near 100% Chance for Thunderstorms

Source: Malaysian Meteorological Department (2009)

2.2 Total Totals Index

Total Totals Index (TTI) is used to forecast the severe local thunderstorm activities and the arithmetic combination of Vertical Totals Index (temperature at 850hPa minus temperature at 500hPa) and the Cross Totals Index (dew point at 850hPa minus temperature at 500hPa) (Peppler, 1988). The TTI is formularized as $TTI = T(850hPa) - T(500hPa) + T_d(850hPa) - T(500hPa)$. T and T_d represent the

temperature and dew point temperature at the indicated level (Miller, 1967). The summary of the TTI range that gives an indication of the possibility of thunderstorms forming over the region is described in Table 2.

Table 2. TTI criteria index range.

TTI	Thunderstorm Potential
< 43	Unlikely
45 – 50	Thunderstorms Possible
50 – 55	Thunderstorms more likely (some severe)
55 – 60	Severe Thunderstorms Likely

Source: Malaysian Meteorological Department (2009)

2.3 Showalter Index

Showalter Index (SI) is used to forecast the non-severe thunderstorm activities over the region. The index estimates the potential instability of the 850hpa to 500hpa layer by measuring the buoyancy at 500hpa of an air parcel lifted to that level (Peppler, 1988). The SI is formularized as $SI = T(500hPa) - T_p(500hPa)$. T_p is the 500hpa temperature that a parcel will achieve if it is lifted dry-adiabatically from 850hpa to its condensation level and then moist-adiabatically to 500hpa (Showalter, 1953). The summary of the SI range that gives an indication of the possibility of thunderstorms forming over the region is described in Table 3

Table 3. SI criteria index range.

SI	Thunderstorm Potential
> 4	Unlikely
+3 to +1	Thunderstorms Possible But Strong Trigger Needed
0 to -3	Moderately Unstable
-4 to -6	Very Unstable, Good Potential of Heavy Thunderstorms
< -6	Extremely Unstable

Source: Malaysian Meteorological Department (2009)

2.4 Lifted Index

Lifted Index (LI) is used as a predictor of latent instability to aid the forecasting of severe local storms at any region of interest. The LI is defined by lifting the parcel adiabatically from the mid-point of the surface layer to 500hpa, where its temperature (T_p at 500hpa), considered to be the updraft temperature within a developing cloud, was compared to that of the environment (Peppler, 1988). The LI is formularized as $LI = T(500\text{ hPa envir}) - T(500\text{hPa parcel})$ (Galway, 1956). Where, $T(500\text{ hPa envir})$ represents the 500 hPa environmental temperature and $T(500\text{hPa parcel})$ is the rising air parcel's 500 hPa temperature. The summary of the LI range that gives a general indication of the strength of convection likely over the region is described in Table 4.

Table 4. LI criteria index range.

LI	Thunderstorm Potential
Positive Value	Unlikely (Stable)
0 to -3	Marginally Unstable
-3 to -6	Moderately Unstable
-6 to -9	Very Unstable
< -9	Extremely Unstable

Source: Malaysian Meteorological Department (2009)

2.5 CAPE Index

Convective Available Energy (CAPE) is the amount of energy that a parcel of air would have if it is lifted to certain distant vertically through the atmosphere or integrated value (Moncrieff et al., 1976). The parcel is lifted until its temperature becomes equal to the temperature of the surrounding environment. The formula used to measure CAPE is as follows;

$$CAPE = GRAVITY * SUMP[DELZ * (TP - TE)/TE]$$

Where, SUMP is the sum over sounding layers from LFCT to EQLV for which (TP - TE) is greater than zero, DEZL is incremental depth, TP is the temperature of a parcel from the lowest 500 m of the atmosphere, raised dry adiabatically to the LCL

and moist adiabatically thereafter and TE is the temperature of the environment. The information is retrieved from <http://weather.uwyo.edu/upperair/indices.html>.

2.6 Linear relationship analysis

The relationship between two quantitative variables of the index is visualized using the scatter plots to describe the general pattern between them. The plot provides an idea if there is a positive or negative association between those indices. Measuring the strength of a relationship from the scatter plots is however quite tricky and requires other numerical measures to support the result. Correlation can be used to measure the strength of a linear relationship between both indices. The statistical metrics such as correlation coefficient (r) is referred to a number that quantifies the relationship between the two indices at the statistical value range between -1 and 1. The closer r is to 0, the weaker the relationship between them. The closer r is to -1 or 1 the stronger the relationship between two indices. Only the scatter plots with strong linear relationship is discussed in this study.

2.7 Total precipitable water analysis

The presence of water vapor in different air layers of the atmosphere is fundamental in meteorological and hydro-meteorological studies. Vertical integrated moisture has a large effect on atmospheric temperature conditions. Atmospheric water vapor originates from the earth's surface therefore it is concentrated in the lower layers and normally about half of its total is found below the level of 2 km (~800 mb). The amount of water vapor in a vertical column of air is given by the Total Precipitable Water (TPW) and defined as the depth of water which would accumulate if all the water vapor in that column was condensed (Viswanadham, 1981). The presence of TPW during the presence of TSRA and FAIR weather condition at the respected stations is analyzed in this study.

3. Data

Hourly thunderstorm data recorded in Meteorological Aviation Report (METAR) is used to represent the current atmospheric condition at both stations. The atmospheric condition was best referred to the stability condition from the index as discussed in section 2. The different thunderstorm patterns and frequency at both

stations are expected to be observed as they are situated 703 km away from each other.

3.1 Thunderstorm data and intensity

Surface observation data from 2010 to 2015 are used in the study. The presence of thunderstorm activities recorded in an one-hour METAR under the present weather codes 13, 17, 29, 91, 92, 95 and 97 was applied to represent the past and present weather phenomena for the stations and the corresponding radius. The details of the present weather code by World Meteorological Organization (WMO) Present Weather Code 4677 (<https://www.nodc.noaa.gov>) are described in Table 5. Thunderstorm intensity is represented by its frequency or total hours of precipitation at certain period of time.

Table 5. Present weather code used in the study.

Code	Present Weather Recorded in METAR
13	Lightning visible, no thunder heard
17	Thunderstorm, but no precipitation at the time of observation
29	Thunderstorm (with or without precipitation) during the preceding hour but not at the time of observation
91	Slight rain at the time of observation. Thunderstorm during the preceding hour but not at the time of observation
92	Moderate or heavy rain at the time of observation. Thunderstorm during the preceding hour but not at the time of observation
95	Thunderstorm, slight or moderate, without hail but with rain and or snow at the time of observation.
97	Thunderstorm, heavy, without hail but with rain and or snow at the time of observation

Source: World Meteorological Organization (WMO) Present Weather Code 4677

3.2 Radiosonde data

The stability index derived from the radiosonde data at 00UTC observation was retrieved from the website (<http://weather.uwyo.edu/upperair/sounding.html>). This is assuming that the stability index is always accurate to represent the actual atmospheric conditions at both stations. Hence, the observed precipitation at the stations is assumed to be manifested due to the current instability situation. The stability index data from Brunei meteorological station (WBSB) is used to represent the atmospheric condition over Miri.

The TSRA phenomenon is identified from METAR data under the present weather codes of 29, 91, 92, 95 and 97 as described in Table 5 above. The sets of stability index were extracted from the radiosonde data with respect to the days of TSRA occurrence. There were 474 days of TSRA that occurred in WBGG with at least 3 hours in frequency. At least 1 hour of TSRA frequency is chosen to represent the actual weather condition over WBGR. A smaller number of TSRA activities were found over WBGR as compared to WBGG. FAIR weather condition at both stations is decided based on METAR that is free from any weather phenomenon that day. Total stability indices data used in the study is described in Table 6.

Table 6. Total stability index data used in the study

Station	TSRA (days)	FAIR (days)
WBGG	474	222
WBGR	279	344

4.0 Result and Discussion

4.1 Thunderstorm analysis pattern

Thunderstorm activities were found to be dominant in WBGG than in WBGR for the entire period of observation as shown in Figure 2. The highest TSRA recorded was 156 days in 2012 while 39 days was recorded as the lowest in WBGR in 2010 and 2014. Maximum TSRA frequency was recorded at 305 hours in WBGG in 2012 and WBGR at 125 hours in 2015. There was no significant drop in the TSRA pattern and frequency in WBGG during the El-Nino year in 2015; however, the frequency was recorded as the highest in WBGR. TS activities were recorded the highest in WBGG

at 119 days in 2012 while WBGR at 86 days in 2015. Total hour of observation for TS in WBGG was recorded higher at 186 hours in 2012 while WBGR at 135 hours in 2015.

The presence of CB clouds over the stations has the potential to induce TSRA and TS at both stations. The record showed that CB has developed over WBGG in 2010 for 321 days consisting of 1774 hours of observation. TSRA and TS frequencies were relatively low despite the enormous CB developed in WBGR. CB cloud was found to be active over WBGR in 288 days in 2015; however, comparatively it contributed less TSRA over the region than in WBGG.

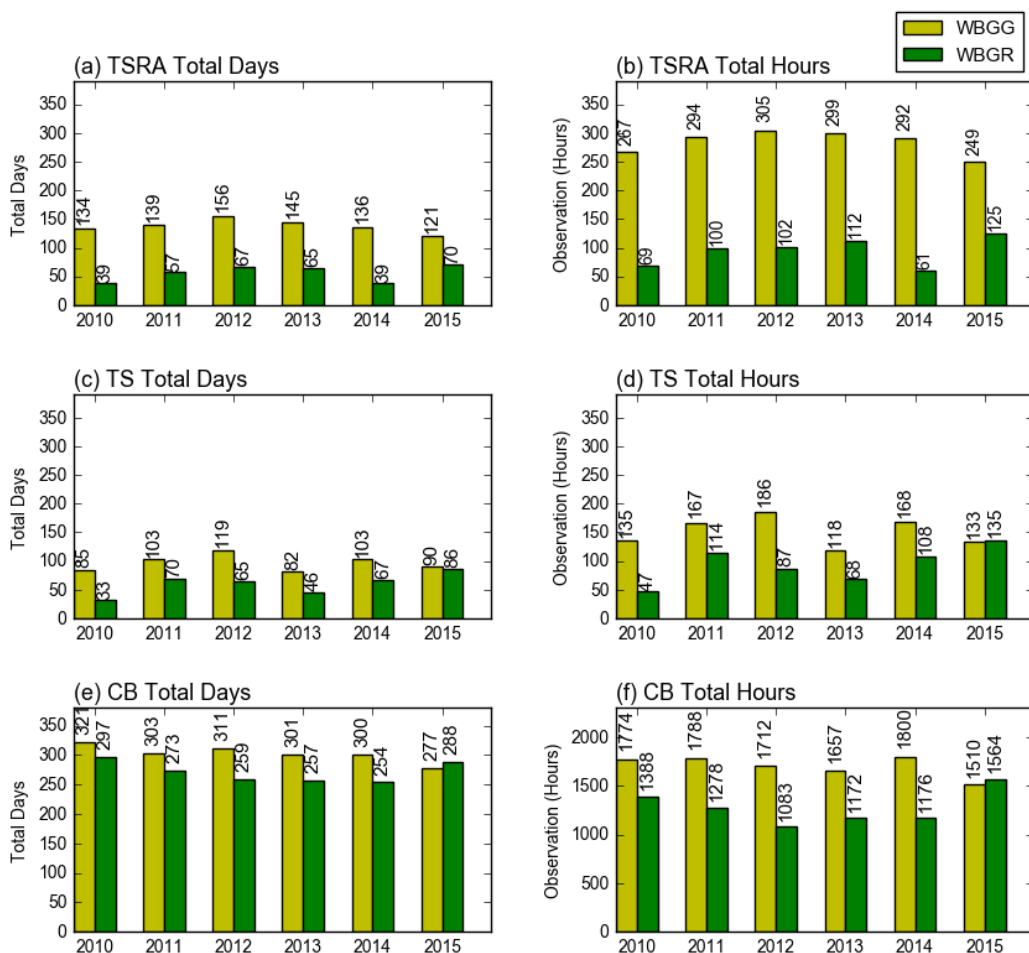


Figure 2. Thunderstorm yearly pattern in WBGG and WBGR

Figure 3 showed the analysis of the hourly distribution of the phenomenon over WBGG and WBGR. TSRA time occurrence in WBGG was sharply increased to its peak at 1700LT while no significant pattern was found in WBGR. The highest frequency of TSRA in WBGG was recorded at 50 hours in 2013 and the lowest was found in 2015 as shown in Figure 3(a). TS activities and pattern in WBGR were clearly defined and compared to TSRA. The highest TS frequency was recorded

between 1400LT and 1600 LT in 2015 at 20 hours observation depicted in Figure 3(d). Generally the TS in WBGG was higher than in WBGR. The highest frequency was recorded in 2012 at the peak in between 1600LT and 1700LT in Figure 3(c). CB pattern at WBGG was maximum at 1700LT at 200 hours' observation in Figure 3(e). The second peak observation was found at 2000LT before it became stable. Two peaks of CB activities were also found in WBGR but slightly different at the time observation than in WBGG. The atmospheric instability in WBGG was slowly depressed than in WBGR when the CB was still found active during late night towards early morning as shown in Figure 3(e) and 3(f).

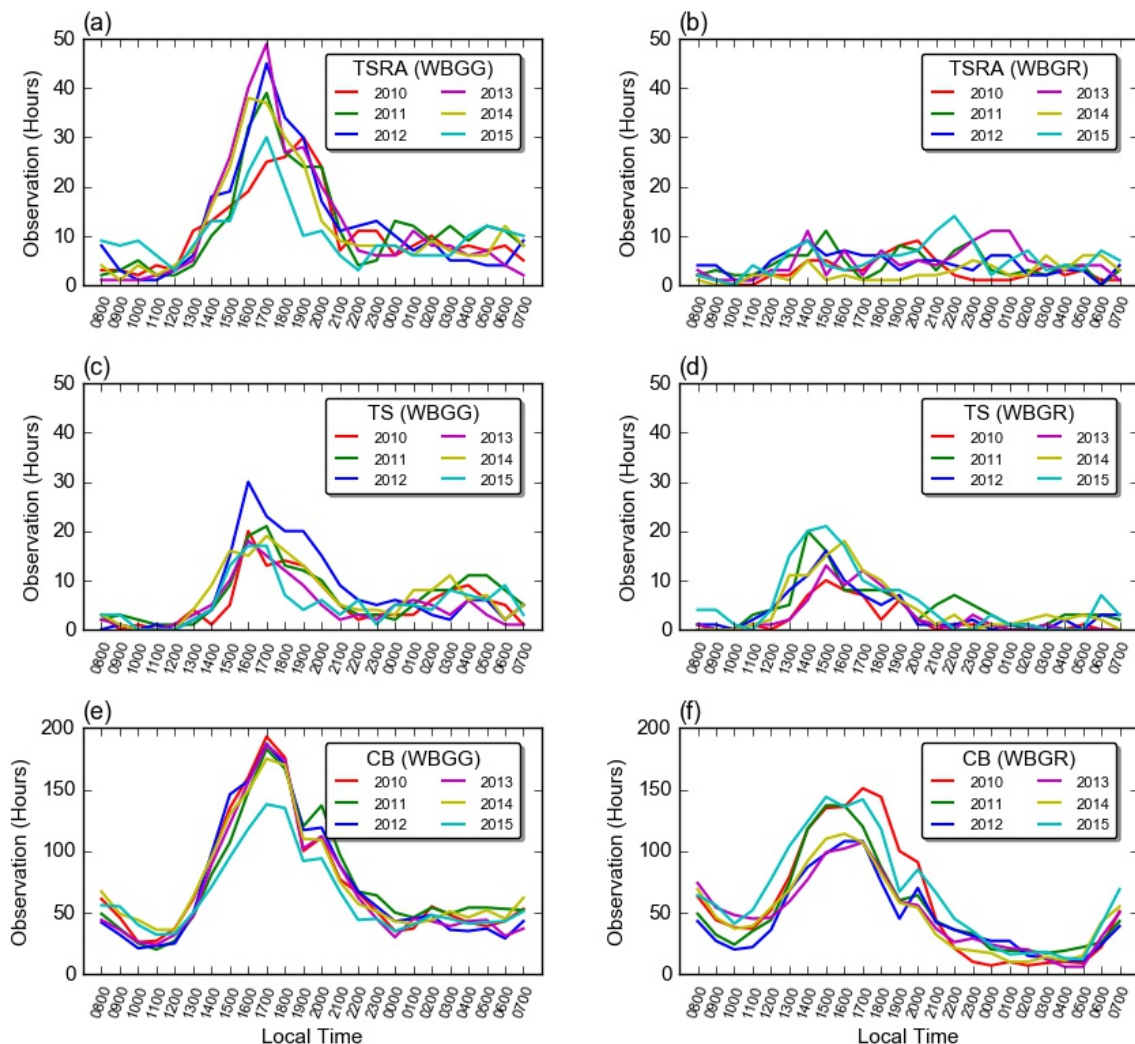


Figure 3. Thunderstorm hourly pattern in WBGG and WBGR

The TSSRA monthly trend in *Figure 4* showed different patterns in both WBGG and WBGR. TSRA in WBGG was found to be so active during the northeast

monsoon and inter-monsoon while slightly depressed in the southwest monsoon. The phenomenon over WBGR was found to be active during the southwest monsoon in 2010 depicted in Figure 4(a) while depressed during the inter- and northeast monsoon. During the late northeast monsoon in 2013 TSRA in Figure 4(e) was found to be smaller at both stations. TSRA in WBGG was generally active than in WBGR for the entire period of study.

TS pattern for both stations was found to be almost similar except in WBGR when the frequency dropped during the southwest monsoon in 2012 as depicted in *Appendix 1*. The pattern showed that the TS frequency was relatively low at both stations in 2010 and 2013. The phenomenon also showed a smaller event during the late northeast monsoon in 2013. The present CB activities as depicted in *Appendix 2* at both stations were almost similar in frequency; however it slightly dropped during the southwest monsoon in 2012 and late northeast monsoon in 2013 which explains why TSRA and TS activities were recorded less in the particular years.

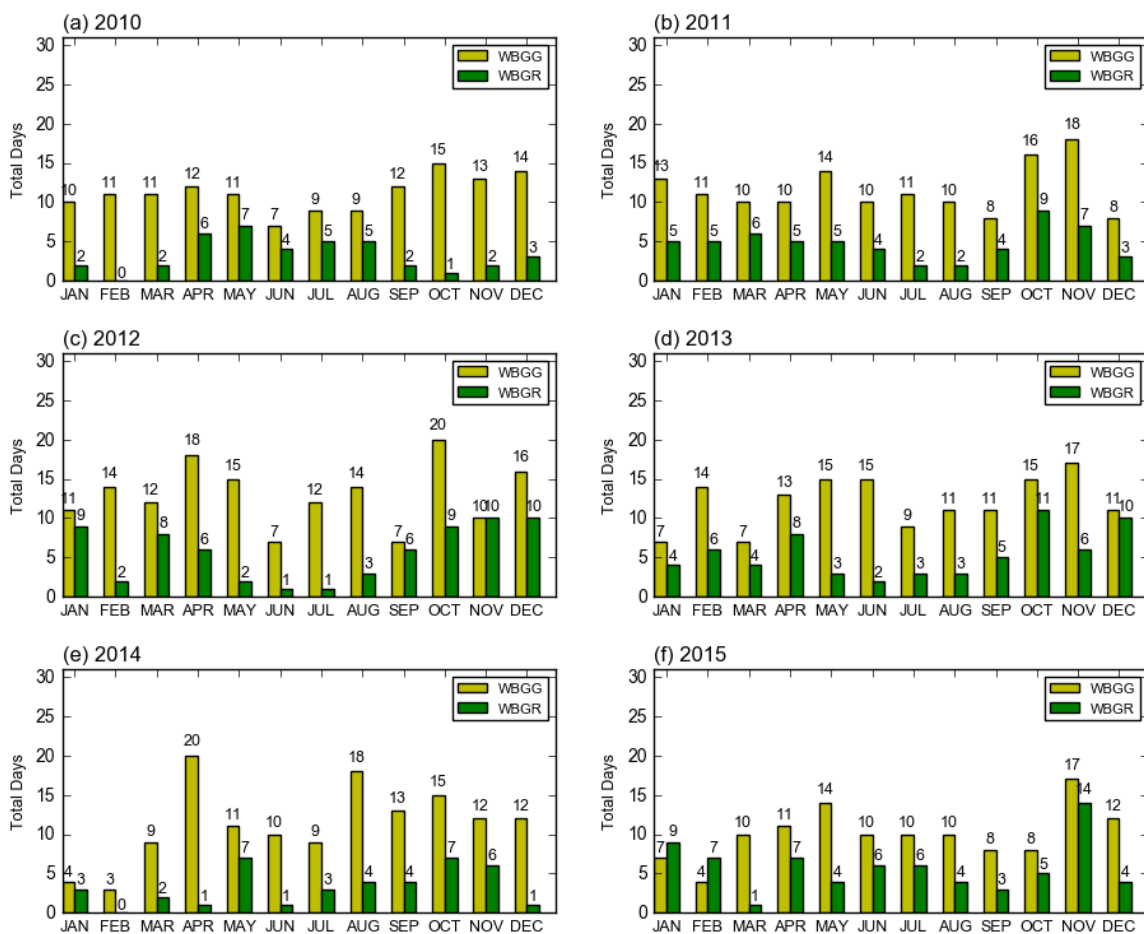


Figure 4. TSRA monthly pattern over WBGG and WBGR

4.2 Stability index analysis

Sets of stability indices during TSRA and FAIR weathers were randomly selected at equal number of 221 observation days (N) for comparison. The stability index was grouped into its classes and presented in the form of two axes of the histogram. Each bar represents the total number of days of the phenomenon at each respected index. TSRA frequency at each index was plotted in order to evaluate how severe the phenomenon was.

4.2.1 K index analysis

Most of the TSRA activities occurred above index 30 and 26 in WBGG and WBGR respectively. Some phenomena even occurred below index 20 but it is small in intensity. The index range depicted in *Figure 5* was fairly distributed according to the model as discussed in section 2.1. The highest frequency of TSRA was recorded at index 34 in both WBGG and WBGR at 133 hours and 75 hours' observation respectively.

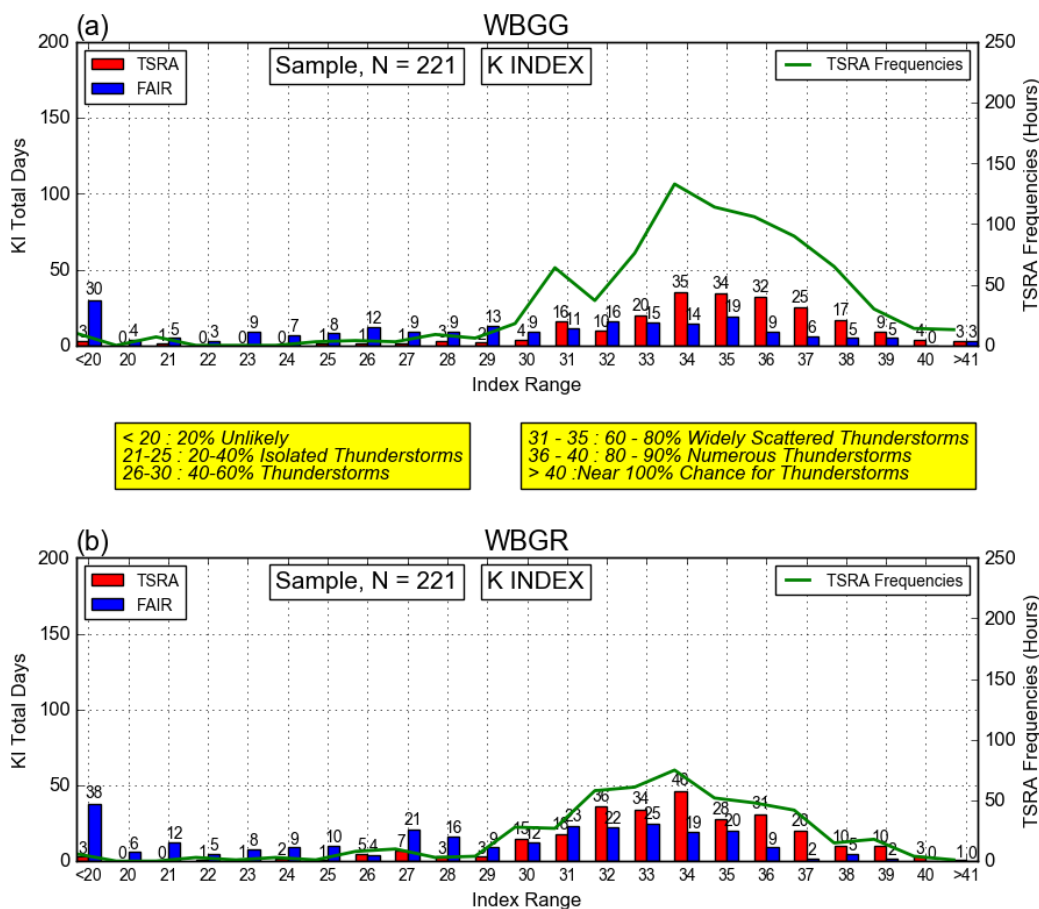


Figure 5. KI index analysis for WBGG and WBGR

4.2.2 Total totals index analysis

TSRA activity for both locations was recorded far less the limit by the stability models discussed in section 2.2. Most of TSRA occurred at below index 48 at *thunderstorms possible* phase at both locations as shown in Figure 6. TSRA was still in the vicinity at an index below 43 although it was located at the *unlikely* phase and appears to be the second highest in frequency at 150 hours in WBGG. TSRA over WBGR was also recorded higher in frequency at 105 hours at *unlikely* phase below 43. The overall highest TSRA frequency occurred at index 44 at both stations.

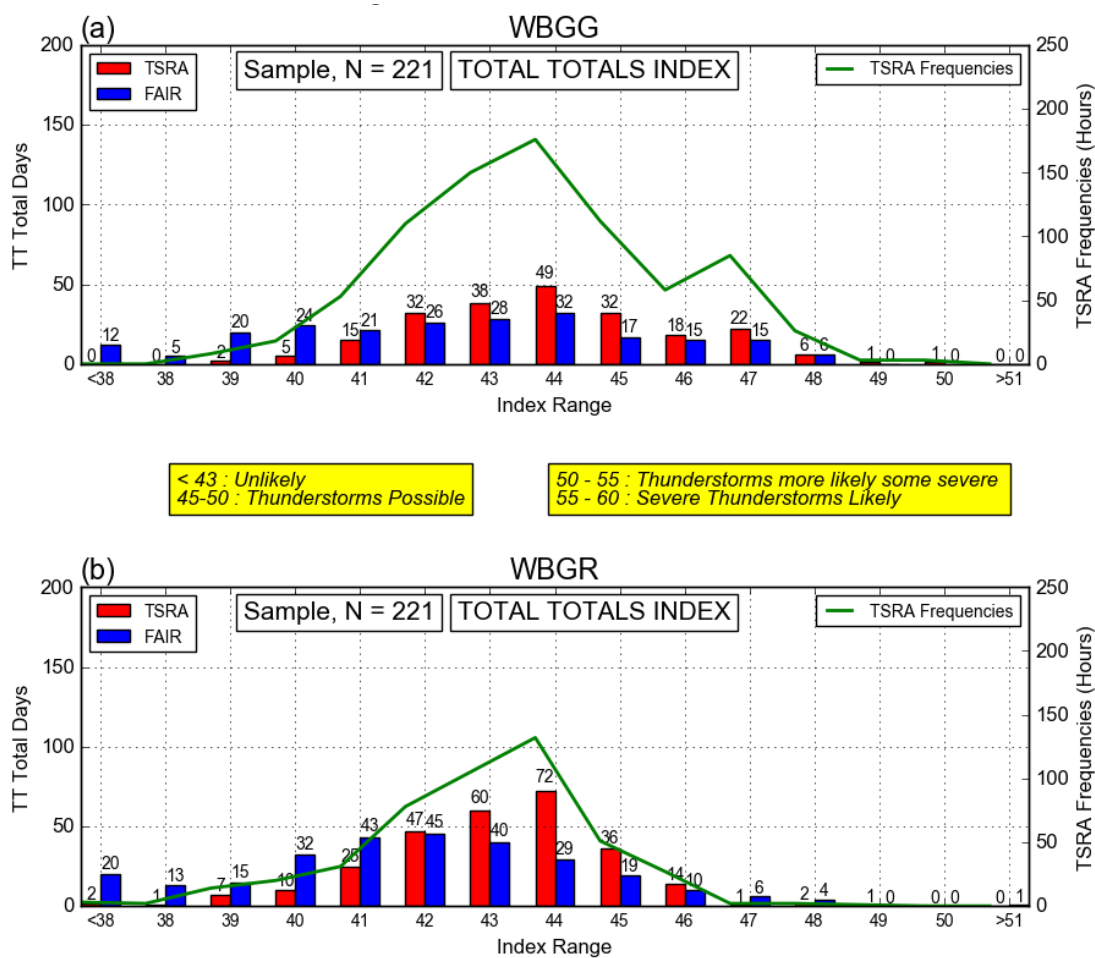


Figure 6. Total totals index (TTI) analysis for WBGG and WBGR

4.2.3 Showalter index analysis

TSRA activity at both stations was almost matched with the model at range *moderately unstable* as shown in Figure 7. The highest frequency of TSRA occurred at

index -1 at both stations. The highest frequency was observed in WBGG at 234 hours within 62 days of observation. The highest frequency of TSRA at WBGR was however smaller than in WBGG at 161 hours of observation within 90 days of observation. The phenomenon over WBGR was still in the vicinity at *unlikely* phase but at a smaller frequency.

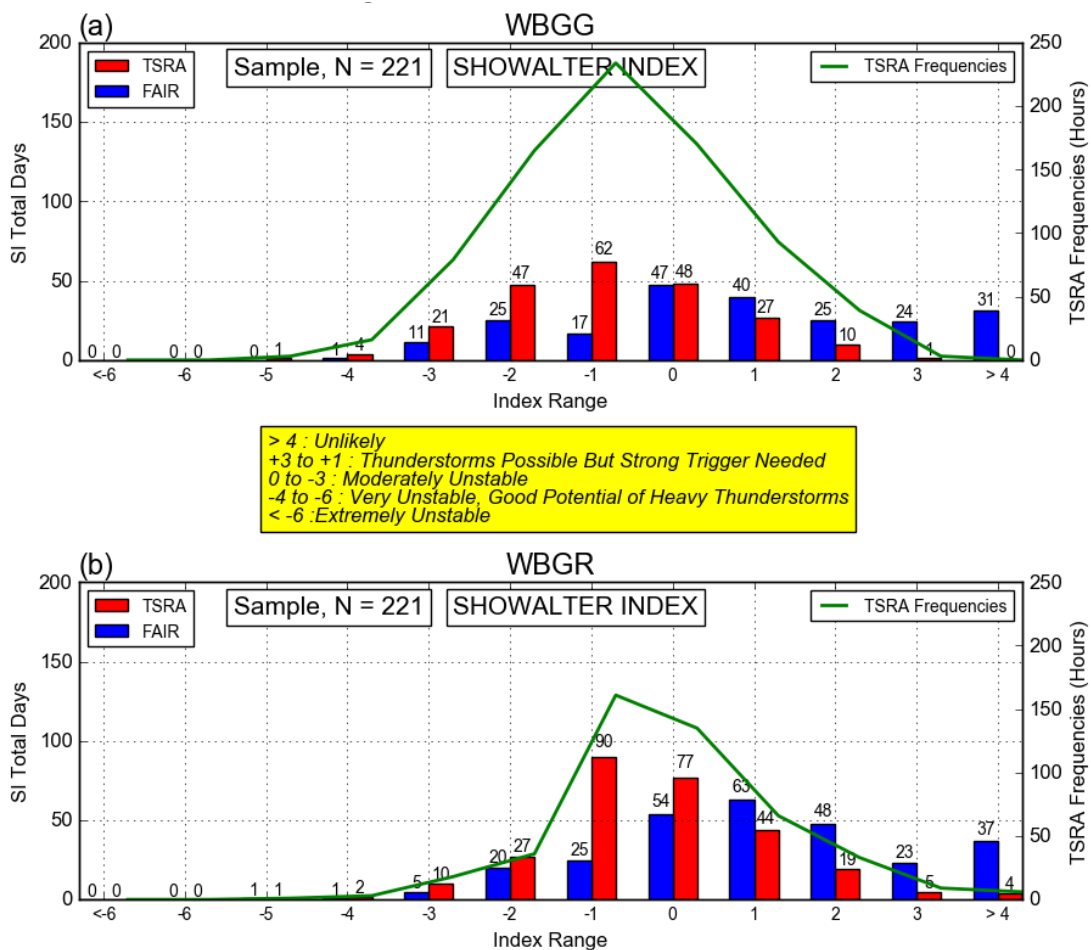


Figure 7. Showalter Index (SI) analysis for WBGG and WBGR

4.2.4 Lifted index analysis

A lifted index in Figure 8 also showed that the TSRA at both locations was well distributed as suggested in the model. The highest frequency occurred at index -4 over WBGG at the frequency of 195 hours of observation. The TSRA frequency in WBGR was the highest at index -3 at 140 hours of observation. The number of phenomenon was also found at the *very unstable* phase at both locations but smaller in the frequency and repetition days.

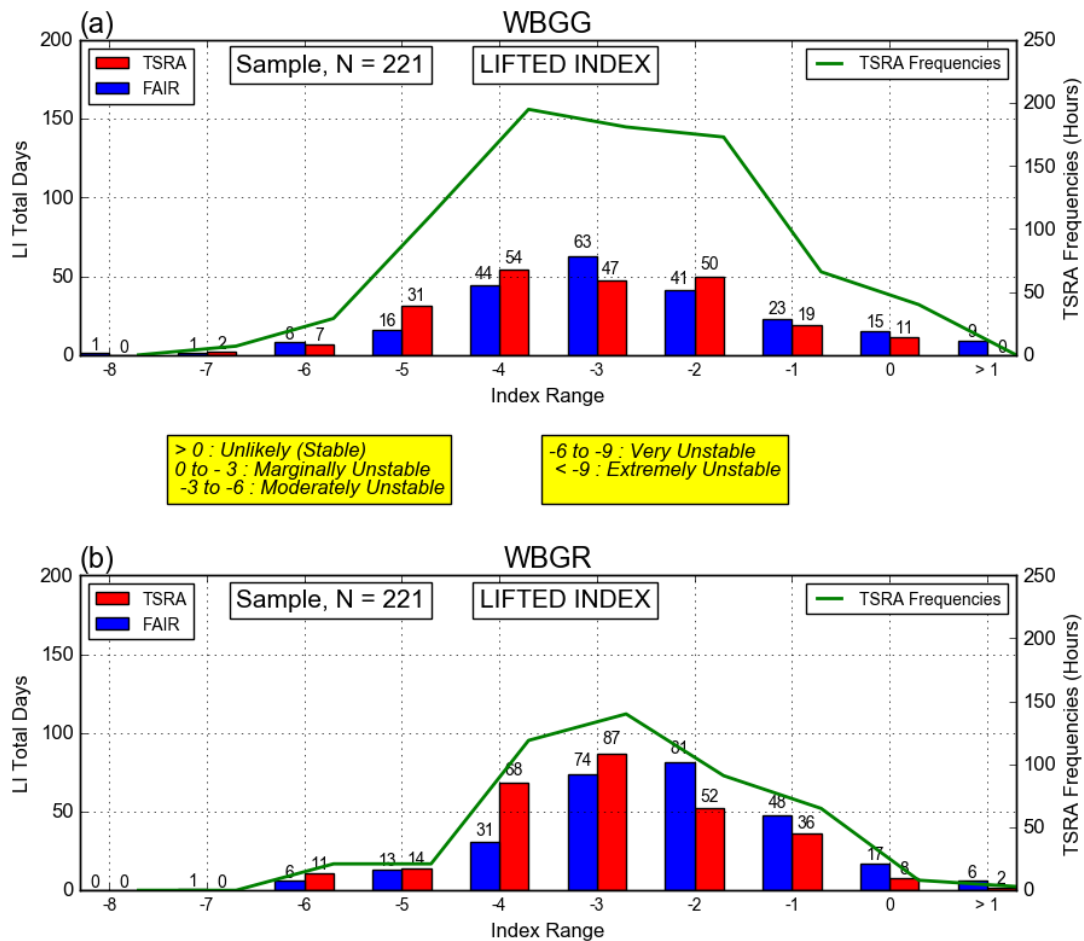


Figure 8. Lifted Index (LI) analysis for WBGG and WBGR

4.3 Linear relationship analysis

Sets of scatter plots of two dimensional indices have been performed to study the linear relationship between them. Monitoring using a single index alone may not be effective to make forecast because the TSRA development over tropics is involved in many factors such as intense surface heating, advection and other localized factors. In order to understand how the index will react towards the atmospheric conditions, two dimensional relationships of the respected index have been observed.

Figure 9 showed the linear relationships between two different indices manifested during TSRA and FAIR in both stations. Red dots show higher intensity of index distribution for the entire observation period. A strong linear relationship between SI and TTI at higher correlation coefficient in between -0.91 and -0.95 is depicted in Figure 9(c), 9(f), 9(i) and 9(l). The negative linear relationship indicates that TSRA will occur if TTI and SI are higher and lower respectively, or vice-versa. The CAPE and LI relationship in Figure 9(b), 9(e), 9(h) and 9(k) was also found to be

in a negative relationship between -0.59 and -0.81. The negative linear relationship indicates that TSRA will occur if CAPE and LI are higher and lower respectively, and vice-versa. The relationship between TPW and KI, however, was found to be positive in the linear relationship between 0.65 and 0.78 in the correlation coefficient as depicted in Figure 9(a), 9(d), 9(g) and 9(j) at both stations. The positive linear relationship indicates that TSRA will occur if both TPW and KI are increased. The linear relationship pattern during FAIR weather as shown in Fig. 9(a), 9(e), 9(f), 9(j), 9(k) and 9(l) was generally similar with TSRA which indicated that the index was not exclusive at any weather situations. The situation makes the prediction of the TSRA activity at stations even more difficult.

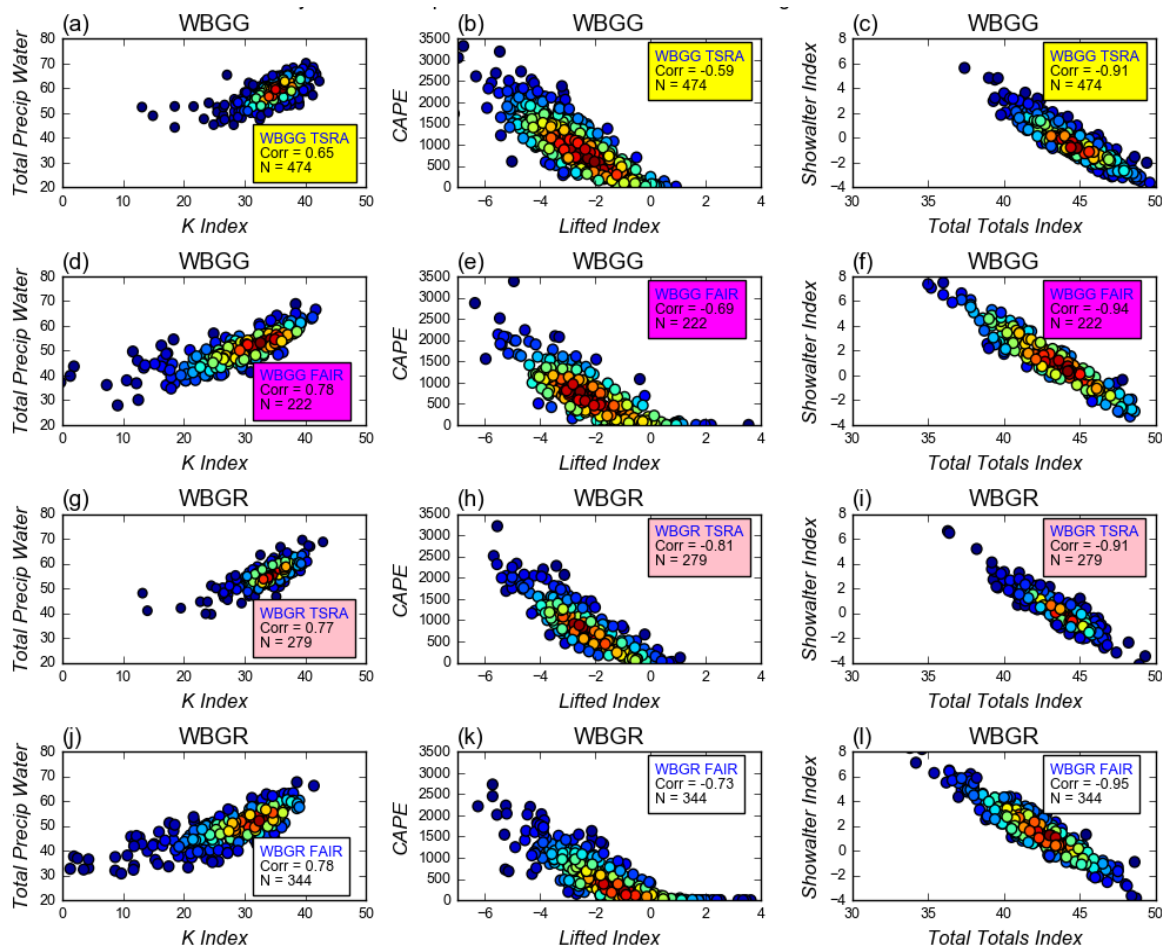


Figure 9. Stability index linear relationship for both WBGG and WBGR

4.3.1 Total precipitable water analysis

The stability index between TSRA and FAIR weather in Figure 9(a), 9(d), 9(g) and 9(j) illustrates some patterns in its density distribution. The index density during

TSRA weather was concentrated at some value range even at a larger dataset. The index density distribution during FAIR weather, however, scattered away even at the smaller data set. TPW may become the third dimension index to support the linear relationship between SI-TTI and CAPE-LI as discussed in 4.3 above. *Figure 10* shows the TPW or water content of the vertical column in the atmosphere observed by the radiosonde. The figure shows that almost 87 hours of TSRA were at the maximum in WBGG when the TPW was at 60mm.

The relationship shows that the higher the water content, the higher the TSRA but lesser in FAIR. TSRA frequency started to increase when the TPW increased from 50mm in WBGG and dominated the station after 55mm before FAIR started to decrease. The TSRA frequency in WBGR started to take place after 45mm and reached the maximum at 55mm in TPW. TSRA began to dominate the station after 53 mm in TPW while FAIR weather was slowing down. TSRA in WBGG and WBGR was still in the vicinity below 49mm and 45mm in TPW respectively but was smaller in frequency.

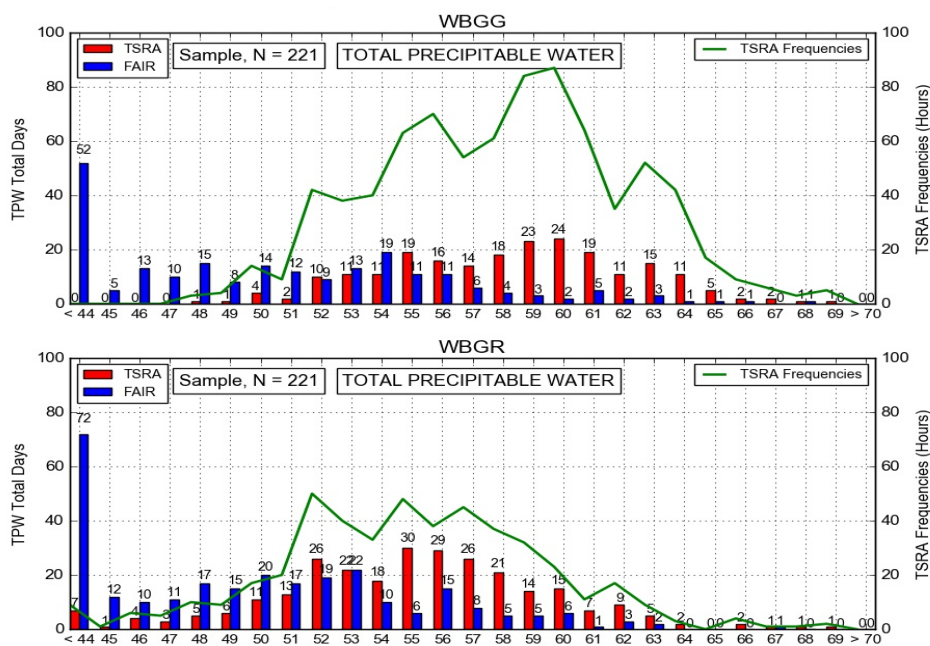


Figure 10. Total precipitable water analysis for WBGG and WBGR

5. Conclusion

TSRA and TS over WBGG dominated the region when the phenomenon was recorded higher at both total number of days and frequency for the entire observation period. The presence of CB cloud activities in WBGR was higher but it

induced smaller TSRA. TSRA in WBGG was found to be the highest when it was recorded for 156 days at 305 hours in frequency during the moderate La-Nina years in 2012. The presence of strong El-Nino years in 2015 however promoted higher TSRA and TS activities in WBGR. The northeast monsoon is found to be the most active season for TSRA and TS occurrences at both stations. TSRA hourly pattern in WBGG was clearly defined in the afternoon at the highest peak of 50 hours of observation at 1700LT while no pattern was found for WBGR. The stability analysis shows that the index is very well distributed according to the model except TTI. Both stations show that a phenomenon occurred even below the *unlikely* phase while sharing the maximum frequency index at 44. The TSRA distribution under KI shows that the phenomenon was distributed at *Widely Scattered* and *Numerous* phases within index 30 to 40. The phenomenon at both stations also shared maximum frequency at index 34 and still occurred below the *unlikely* phase but minimal in frequency. The highest TSRA frequency in SI occurred at the *Moderately Unstable* phase at both stations. The higher percentage of TSRA was induced at index -1 when total days of FAIR weather were recorded smaller than in TSRA. From the LI analysis the index was shown to be concentrated at *Marginally Unstable* and *Moderately Unstable*. Forecasting using a single index was challenging because the index was not exclusively representing the single phenomenon. TSRA and FAIR weather can be manifested even when the atmospheric condition was not in favorable to occur.

The statistics shows that the number TSRA and FAIR at the respected index was almost equal. The linear relationship analysis of two dimensional indices was performed to observe how certain indices reacted to each other in linear form and to provide the limit and scope to perform the forecast. A strong linear relationship was found in among TPW-KI, CAPE-LI and SI-TTI as shown in the scatter plot. TPW-KI was found to be in a positive linear relationship while CAPE-LI and SI-TTI were at a negative relationship. The index density distribution for TPW-KI shows some unique patterns as shown in Figure 9(a), 9(d), 9(g) and 9(j). The index density during the TSRA weather is concentrated at some value range even at larger dataset while scattered away during FAIR at smaller data set. The relationship shows that the higher the water content, the higher the TSRA frequency but lesser in FAIR weather.

6. Acknowledgement

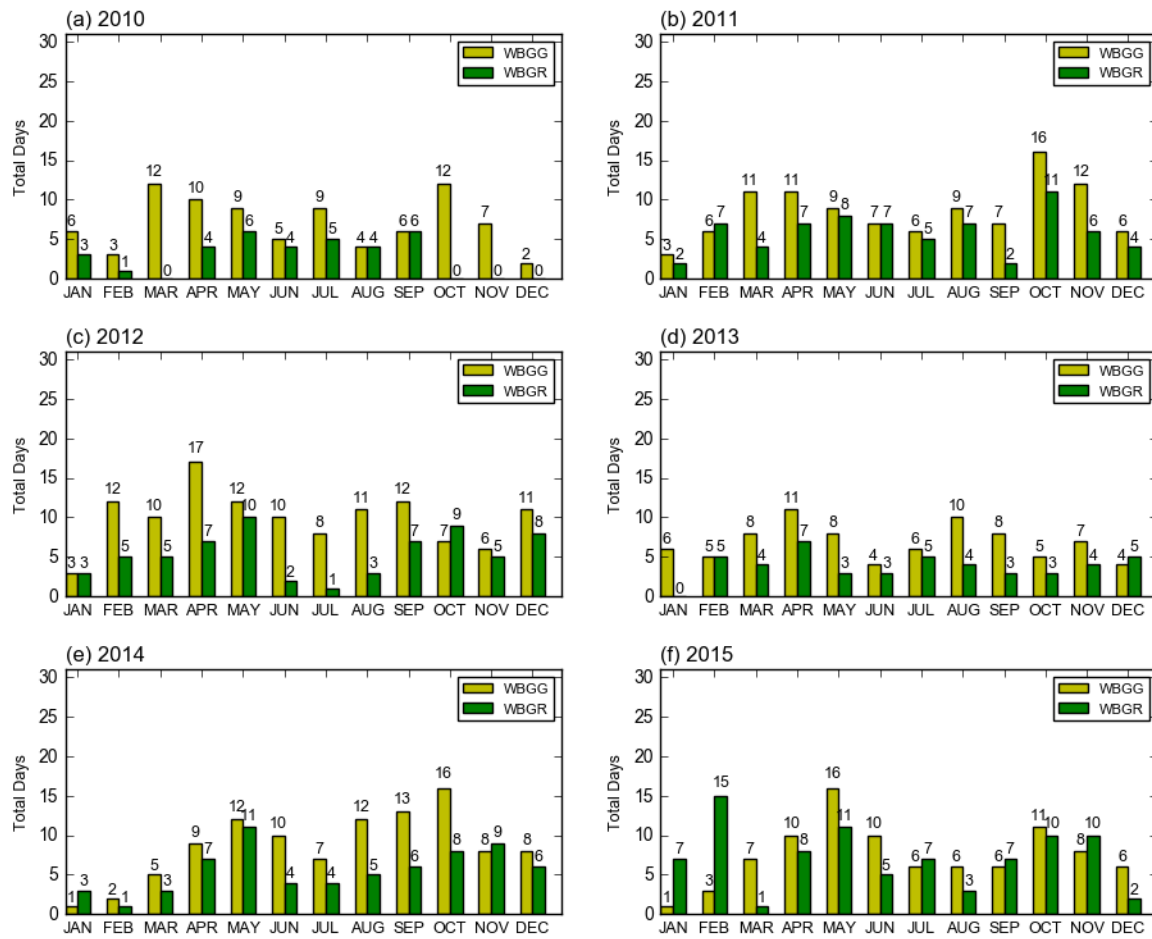
Special thanks to the Sarawak Meteorological Office and National Climate Center of Malaysian Meteorological Section (MMD) for contributing to the success of this study.

References

- Atmospheric Sounding. (2017). Retrieve from <http://weather.uwyo.edu/upperair/sounding.html>
- Bhattacharya, R., & Bhattacharya, A. (2011). Stability parameters and their skill to forecast thunderstorm. *International Journal of Physics*, 4 (1), 21 – 30.
- Galway, J. G. (1956). The lifted index as a predictor of latent instability. *Bulletin of the American Meteorological Society*, 37, 528 – 529.
- George, J. J. (1960). *Weather forecasting for aeronautics*. New York and London Academic Press, 407-415. Retrieved from <https://books.google.com.my>
- Gottlieb, R. J. & Wysocki, M. W. (2009). *Analysis of stability indices for severe thunderstorms in the Northeastern United States* (Unpublished master's thesis). Cornell University. <https://core.ac.uk/download/pdf/79022869.pdf>
- Malaysian Meteorological Department. (2010). *Training section, synoptic observation codes (SYNOP, METAR & SPECI)*, Present Weather Code 4677.
- Malaysian Meteorological Department. (2009). *Forecasting guide manual*. Nowcasting/Short Range Forecasting, 52 – 58.
- Miller, R. C. (1967). Notes on analysis and severe storm forecasting procedures of the Military Weather Warning Center. *Tech. Report 200*, AWS, USAF. [Headquarters, AWS, Scott AFB, 1L 62225]
- Moncrieff, M. W. & Miller, M. J. (1976). The dynamics and simulation of tropical cumulonimbus and squall lines. *Quarterly Journal of the Royal Geographical Society*, 102, 373 – 394.
- Peppler, R. A. (1988). *A review of static stability indices and related thermodynamic parameters*. Illinois State Water Survey Miscellaneous Publication 104: 87. Retrieved from <https://www.isws.illinois.edu/pubdoc/MP/ISWSMP-104.pdf>
- Radiosonde Observation. (2017). Retrieved From <http://www.weather.gov/upperair/factsheet>.

- Shaari, N. A., Omar, A. R., Mat, T. M. A., Saad, M. S., Mohd Ludi, A. K., & Abd. Ghani, N. S. (2015). Study case: Study on data sounding sensitivity towards thunderstorm activities over Peninsular Malaysia during inter monsoon period from 2010 to 2014. *Malaysian Meteorological Department*, ISBN/ISSN: ISBN: 978-967-5676-69-7.
- Showalter, A. K. (1953). A stability index for thunderstorm forecasting. *Bulletin of the American Meteorological Society*, 34, 250 – 252.
- Stull, R. (2017). *Practical meteorology: An algebra-based survey of atmospheric science*. Retrieved from https://www.eoas.ubc.ca/books/Practical_Meteorology/prmet102/Chapters/Ch14-Tstorm-v102b.pdf
- Thunderstorms Basic. (2017). The National Severe Storms Laboratory. Retrieved from <http://www.nssl.noaa.gov/education/svrwx101/thunderstorms/>
- Viswanadham, Y. (1981). The relationship between total precipitable water and surface dew point. *Journal of Applied Meteorology*, 20 (1), 3 – 8.

Appendix 1. TS monthly pattern over WBGG and WBGR



Appendix 2. CB monthly pattern over WBGG and WBGR

